New Journal of Physics
The open access journal at the forefront of physics

Deutsche Physikalische Gesellschaft DPG
IOP Institute of Physics

Published in partnership with: Deutsche Physikalische Gesellschaft and the Institute of Physics

OPEN ACCESS

RECEIVED
27 February 2015

REVISED
22 April 2015

ACCEPTED FOR PUBLICATION
23 April 2015

PUBLISHED
22 May 2015

PAPER

Quantum theory of collective strong coupling of molecular vibrations with a microcavity mode

Javier del Pino[1], **Johannes Feist**[1] **and Francisco J Garcia-Vidal**[1,2]

[1] Departamento de Física Teórica de la Materia Condensada and Condensed Matter Physics Center (IFIMAC), Universidad Autónoma de Madrid, Madrid E-28049, Spain
[2] Donostia International Physics Center (DIPC), E-20018 Donostia/San Sebastian, Spain

E-mail: johannes.feist@uam.es

Keywords: organic molecules, strong coupling, vibrational modes, polaritons, quantum optics

Abstract

We develop a quantum mechanical formalism to treat the strong coupling between an electromagnetic mode and a vibrational excitation of an ensemble of organic molecules. By employing a Bloch–Redfield–Wangsness approach, we show that the influence of dephasing-type interactions, i.e., elastic collisions with a background bath of phonons, critically depends on the nature of the bath modes. In particular, for long-range phonons corresponding to a common bath, the dynamics of the 'bright state' (the collective superposition of molecular vibrations coupling to the cavity mode) is effectively decoupled from other system eigenstates. For the case of independent baths (or short-range phonons), incoherent energy transfer occurs between the bright state and the uncoupled dark states. However, these processes are suppressed when the Rabi splitting is larger than the frequency range of the bath modes, as achieved in a recent experiment (Shalabney *et al* 2015 *Nat. Commun.* **6** 5981). In both cases, the dynamics can thus be described through a single collective oscillator coupled to a photonic mode, making this system an ideal candidate to explore cavity optomechanics at room temperature.

1. Introduction

The field of cavity optomechanics explores the interaction between electromagnetic (EM) radiation and the quantized mechanical motion of nano- or micro-oscillators [1–3]. Recent developments promise a rich variety of applications such as precision mechanical measurements and coherent control of quantum states (see [4, 5] for recent reviews). When the interaction becomes sufficiently large, coherent energy exchange between the optical and mechanical degrees of freedom becomes possible and the system could reach the strong coupling regime. Along this direction, a novel approach consists in coupling a cavity mode to a molecular bond vibration [6, 7], which is in the ground state already at room temperature, without requiring any cooling. In order to achieve strong coupling, this has to be done by using an ensemble of molecules. This phenomenon has common ingredients with the collective strong coupling observed when electronic excitations of organic molecules interact with cavity [8–10] or plasmonic modes [11], which has been studied extensively during the last years (see [12, 13] for recent reviews).

In the strong coupling with an ensemble of vibrational modes, the cavity resonance couples to a *collective* superposition of the molecular vibrations, the so-called bright state, forming hybrid states called polaritons. In principle, all other superpositions of vibrational excitations (the so-called dark states) remain uncoupled. However, within this setting, a thermal bath of low-frequency rovibrational modes, which normally only introduces dephasing [14, 15], interacts with the vibrational excitations and may influence the system dynamics. It is an open question how the dephasing mechanisms affect the strongly coupled dynamics and what role the dark states play. In particular, it is unknown whether the bright mode in such a system effectively behaves like a single isolated oscillator, which would enable the direct application of protocols developed in cavity optomechanics.

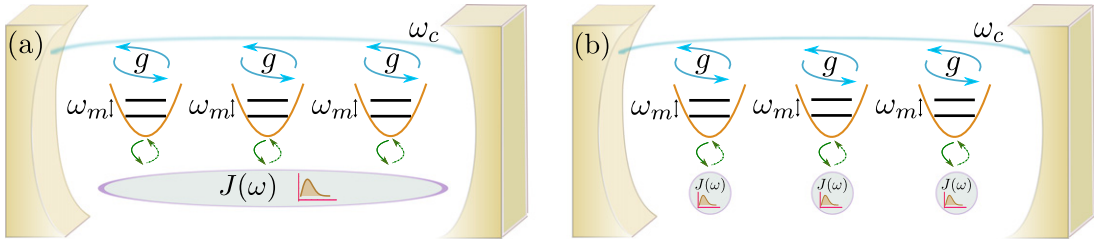

Figure 1. Sketch of the model system. An ensemble of N molecules interacts collectively with a cavity mode of frequency ω_c. The cavity is tuned to a molecular vibrational mode. The remaining rovibrational modes are introduced by either connecting all molecules to a common bath (panel (a)) or by coupling each molecule with an independent bath (panel (b)). In both cases the harmonic bath is characterized by a spectral density $J(\omega)$.

In this paper, we present a fully quantum theory of the phenomenon of collective strong coupling of molecular vibrations with a cavity mode. In contrast to classical transfer matrix calculations, which can be used to fit the experimental spectra [6, 7] but only provide very limited information about the incoherent dynamics in the system, our approach naturally incorporates all incoherent processes, in particular those induced by dephasing-type interactions. We describe the system using a quantum-mechanical model of a single photon mode coupled to an ensemble of harmonic oscillators representing molecular vibrations (the C=O bond stretching mode of polyvinyl acetate at an energy of 215 meV in the experiment [6]). In order to incorporate the coupling of the molecular vibrations to low-frequency rovibrational modes, we assume that the oscillators are connected to either a *common* or to *independent* phononic baths (see figure 1). We employ Bloch–Redfield–Wangsness (BRW) theory [16, 17] to obtain master equations describing the system dynamics under strong coupling. The final master equations only contain a few Lindblad terms, with rates determined by the product of (i) the bath spectral density at the corresponding transition frequency and (ii) algebraic prefactors obtained from transforming the system into its eigenstate basis. Using the specific properties of the system under study, we can evaluate all these prefactors *analytically*, and are thus able to directly read off the population transfer rates between the system eigenstates. This allows detailed insight into the system dynamics and, specifically, the role of the dark states. Our results demonstrate that for large enough Rabi splitting, the bright state indeed behaves like a *single* isolated oscillator and the dark states play an almost negligible role. For the case of a common bath, corresponding to long-range bath phonons, this is even true regardless of the Rabi splitting.

2. Theory

2.1. Coherent dynamics

We model the system as a set of N molecular vibrational modes coupled to a *single* electromagnetic (EM) mode in a microcavity, as depicted in figure 1. The mirrors in the experiments [6, 7] are actually planar, and the photonic modes form a continuum, with a dispersion relation depending on the in-plane momentum $\vec{k}_\parallel$. However, the assumption of a single EM mode coupling to many molecules is justified when comparing the density of EM modes with the molecule density in the experiment. For the jth transversal mode in a cavity of length L with background refractive index n, the momentum perpendicular to the plane mirrors is fixed to $k_\perp = \frac{j\pi}{L}$, so that the dispersion in terms of the (two-dimensional) in-plane wavevector $\vec{k}_\parallel$ is $\omega = \frac{c}{n}\sqrt{k_\parallel^2 + \left(\frac{j\pi}{L}\right)^2}$, (where $k_\parallel = |\vec{k}_\parallel|$). The 2D density of EM modes with wavevector $k_\parallel < k_{\max}$ is $N_{\rm ph} = \frac{1}{4\pi^2}\int_0^{k_{\max}} 2\pi k_\parallel \, {\rm d}k_\parallel = k_{\max}^2/(4\pi)$. Inserting the cavity mode dispersion gives a density of states with energy $\omega < \omega_{\max}$ of (here and in the following, we set $\hbar = 1$)

$$N_{\rm ph}^{(j)} = \frac{n^2}{4\pi c^2}\left(\omega_{\max}^2 - \omega_j^2\right), \tag{1}$$

where $\omega_j = \frac{c}{n}\frac{j\pi}{L}$. We assume that modes with $j = 1$ and $\omega < \omega_{\max} \approx \omega_1 + \Omega_R$ participate in the dynamics. Taking the parameters from the experiment of Shalabney *et al* [6] ($n \approx 1.41$, $\omega_1 = 215$ meV, $\Omega_R = 20.7$ meV, $L \approx 2\,\mu$m), this leads to an EM mode density of $N_{\rm ph} \approx 4 \times 10^6$ cm^{-2}. In contrast, the reported molecular density is $d \approx 8 \times 10^{21}$ cm^{-3}, giving a 2D molecular density of $Ld \approx 2 \times 10^{18}$ cm^{-2}. There are thus on the order of 10^{12} molecular vibrational modes coupled to each photonic mode, and our assumption is clearly justified.

Within the rotating wave approximation, i.e., neglecting processes that create or destroy two excitations, the coherent dynamics of the system is then governed by the Hamiltonian:

$$H_s = \omega_c a^\dagger a + \sum_{i=1}^{N} \omega_i c_i^\dagger c_i + \sum_{i=1}^{N} g_i (a c_i^\dagger + a^\dagger c_i), \tag{2}$$

where a is the annihilation operator for the cavity mode with frequency ω_c, and c_i is the annihilation operator of the optically active vibrational mode of molecule i, characterized by its frequency ω_i and its position $\vec{r}_i$. The cavity-oscillator interaction is given by g_i, which depends on the cavity electric field strength and the change of the molecular dipole moment under displacement from the equilibrium position (see [6] for details). For simplicity, in this work we assume a regular configuration in which all the molecules are identical ($\omega_i = \omega_m$, $g_i = g$), as well as zero detuning ($\omega_c = \omega_m$). Using a direct numerical implementation of BRW theory, which works with arbitrary (but small enough) systems, we have explicitly checked that orientational disorder ($g_i \neq g_j$) and inhomogenous broadening ($\omega_i \neq \omega_j$) do not significantly affect the results presented below.

We focus on the linear response of the system, so that we can restrict the treatment to the zero- and single-excitation subspaces[3]. The $N + 1$ singly excited eigenstates of H_s are formed by: (i) two *polaritons*, $|\pm\rangle$, symmetric and antisymmetric linear combinations of the cavity mode $a^\dagger |0\rangle$, with the collective *bright state* of the molecular excitation, $|B\rangle = \frac{1}{\sqrt{N}} \sum_i c_i^\dagger |0\rangle$; $|\pm\rangle = \frac{1}{\sqrt{2}} (a^\dagger |0\rangle \pm |B\rangle)$ and ii) the so-called *dark states*, $N - 1$ combinations of molecular excitations orthogonal to $|B\rangle$, which have eigenfrequencies ω_m and no mixing with the photonic mode. The eigenfrequencies of the two polariton modes are $\omega_m \pm g\sqrt{N}$, with Rabi splitting $\Omega_R = 2g\sqrt{N}$. Collective strong coupling emerges when Ω_R is larger than the losses of the system. We can distinguish three types of loss mechanisms: cavity losses (rate κ), non-radiative internal losses within the molecules (rate γ_{nr}), and dephasing-type interactions. Spontaneous radiative decay is very slow (on the scale of milliseconds) due to the low transition frequencies and can be safely neglected[4].

2.2. Incoherent dynamics

We now turn to the description of the incoherent dynamics induced by the different loss mechanisms. Whereas cavity losses and nonradiative internal molecular decay can be seen as pure decay channels and included as constant Lindblad terms when analyzing the system dynamics, dephasing-type interactions must be treated in a more detailed fashion, as we detail below. In the case analyzed in this work, these interactions are due to elastic scattering of low-frequency rovibrational bath modes with the main vibrational modes involved in strong coupling, described by the interaction Hamiltonian

$$H_\phi = \sum_{i=1}^{N} c_i^\dagger c_i \sum_k \lambda_{ik} (b_{ik} + b_{ik}^\dagger). \tag{3}$$

The spatial extension or localization of the bath modes determines the character of the coupling. In the following, we focus on two limiting scenarios. In the first scenario, all the vibrational modes are coupled to the same *common* bath (see figure 1(a)), characterized by delocalized phonons $b_{ik} = b_k$ with bath Hamiltonian $H_b^{com} = \sum_k \omega_k b_k^\dagger b_k$. In the second scenario, each molecular vibrational mode is coupled to an *independent* bath characterized by on-site phonons b_{ik}, with bath Hamiltonian $H_b^{ind} = \sum_{ik} \omega_{ik} b_{ik}^\dagger b_{ik}$. In both scenarios, we assume that all molecules are identical ($\lambda_{ik} = \lambda_k$ and $\omega_{ik} = \omega_k$).

The frequently used approach of treating dephasing through a frequency-independent Lindblad superoperator acting only on the vibrational modes is not valid in our case as, within the strong coupling regime, the molecule-cavity coupling (frequency Ω_R) is much faster than the correlation time of the phononic environment (the timescale on which bath correlations decay, i.e., within which the bath 'forgets' about state changes). Instead, the influence of the background modes has to be taken into account in the *dressed* basis obtained after diagonalizing the strong-coupling interaction. The bath is completely characterized by the spectral density $J_i(\omega) = \sum_k \lambda_{ik}^2 \delta(\omega - \omega_{ik})$ (with $J_i(\omega) = J(\omega)$ in our case). In the following, we assume an Ohmic environment with a quadratic cutoff at frequency ω_{cut}

$$J(\omega) = \eta \omega e^{-(\omega/\omega_{cut})^2}, \tag{4}$$

where η is a dimensionless constant that determines the system-bath coupling strength.

[3] We note that since the system Hamiltonian is quadratic in the bosonic modes $\{a, c_i\}$, it can in principle be diagonalized without restriction to any excitation subspace. This leaves most of the derivation presented in the following unchanged, but introduces additional prefactors depending on the excitation numbers in the incoherent rates derived below. For simplicity, we thus allow at most one excitation.

[4] Note that there is no Purcell enhancement of the spontaneous emission, as the effect of the cavity mode is already accounted for by including it as a bosonic degree of freedom in the system Hamiltonian, see, e.g., [18, 19]. The remainder of the photonic spectral density in the cavity is flat and actually suppressed below the vacuum value.

If the system-bath coupling is sufficiently weak, BRW theory [16, 17] can be safely applied to derive a master equation for the system dynamics [20, 21]. This approach relies on the first and second *Born approximation*, which calculate the effect of the system-bath coupling up to second order perturbation theory and assume that the bath state remains unmodified, i.e., the bath density matrix $\rho_{\rm b}$ is time-independent (and thermally populated in the following), where $\rho_{\rm total}(t) \simeq \rho(t) \otimes \rho_{\rm b}$. Additionally, since the decay of the bath correlations ($\sim 1/\omega_{\rm cut}$, see below) occurs on a much shorter time scale than the dynamics caused by the interaction with the bath, the *Markov approximation* is used, disregarding all memory effects of the system-bath interaction. In the interaction picture (denoted by a tilde, $\tilde{O} = e^{i(H_s+H_b)t} O e^{-i(H_s+H_b)t}$), the system density operator $\tilde{\rho}$ then evolves according to

$$\partial_t \tilde{\rho}(t) = -\int_{-\infty}^{t} \mathrm{Tr}_{\rm b}\Big[\tilde{H}_\phi(t), \big[\tilde{H}_\phi(t'), \tilde{\rho}(t) \otimes \rho_{\rm b}\big]\Big] \mathrm{d}t', \tag{5}$$

where $\mathrm{Tr}_{\rm b}$ denotes the trace over the bath degrees of freedom.

The bath-dependent part of the system-bath coupling is fully encoded in the bath *correlation functions* between the modes on molecular sites i and j, $\phi_{i,j}(\tau) = \sum_k \mathrm{Tr}_{\rm b}[\tilde{b}_{ik}^\dagger(\tau)\tilde{b}_{jk}(0)\rho_{\rm b}]$. It is independent of both i and j for a common bath, $\phi_{i,j}^{\rm com}(\tau) = \phi(\tau)$, while for independent baths, the off-diagonal terms vanish, $\phi_{i,j}^{\rm ind}(\tau) = \delta_{i,j}\phi(\tau)$. The *autocorrelation* function $\phi(\tau)$ can be expressed through the spectral density [22]

$$\phi(\tau) = \int_0^\infty J(\omega)\Big\{[n(\omega)+1]e^{-i\omega\tau} + n(\omega)e^{i\omega\tau}\Big\}\mathrm{d}\omega, \tag{6}$$

where $n(\omega) = (e^{\beta\omega} - 1)^{-1}$ is the Bose occupation factor and $\beta = 1/k_{\rm B}T$, with $k_{\rm B}$ the Boltzmann constant and T the temperature. In the high-temperature limit $\beta\omega_{\rm cut} \gg 1$, it can be shown that $\phi(\tau) \propto \exp\{(-\omega_{\rm cut}^2 t^2)/4\}$, i.e., the bath correlation time is $\sim 1/\omega_{\rm cut}$.

We now evaluate equation (5) within the system eigenbasis. Before we proceed, we note that the common approach of using frequency-independent Lindblad terms to describe dephasing is equivalent to neglecting the strong coupling in the incoherent dynamics, i.e., to use only the uncoupled system Hamiltonian $\omega_c a^\dagger a + \omega_m \sum_i c_i^\dagger c_i$ in the interaction picture on the right-hand side of equation (5). When the molecule-cavity coupling is comparable to or faster than the decay of bath correlations ($\Omega_R \gtrsim \omega_{\rm cut}$), this is an invalid approximation, and it is crucial to include the full system Hamiltonian when deriving the master equation to satisfy detailed balance [23]. This point was also stressed in a recent paper in the context of electronic strong coupling [24], based on a phenomenological model of the system.

We thus proceed by expressing the system part of H_ϕ ($\propto c_i^\dagger c_i$) in terms of the dressed eigenbasis (where $H_s|a\rangle = \omega_a|a\rangle$) and inserting this expansion in equation (5). This leads to

$$\partial_t\tilde{\rho} = \sum_{i,j=1}^{N}\sum_{p,q,r,s}\int_0^\infty \phi_{ij}(\tau)\,u_{ip}u_{iq}u_{jr}u_{js}\,e^{i(\omega_{pq}-\omega_{sr})t + i\omega_{sr}\tau}\Big[\sigma_{rs}\tilde{\rho}(t), \sigma_{pq}\Big]\mathrm{d}\tau + \mathrm{h.c.}, \tag{7}$$

where $\sigma_{ab} = |a\rangle\langle b|$, $\omega_{ab} = \omega_a - \omega_b$, and the sums over p, q, r and s include all system eigenstates. Furthermore, $u_{ia} = \langle a|\, c_i^\dagger\, |0\rangle$ give the overlaps between system eigenstates and vibrational mode excitations and can be chosen real. Finally, we made the substitution $t' = t - \tau$. Inserting $\phi(\tau)$ from equation (6) leads to integrals of the type

$$\int_0^\infty e^{\pm i\Delta\omega\tau}\mathrm{d}\tau = \pi\delta(\Delta\omega) \pm i\,\mathrm{P.V.}(\Delta\omega^{-1}), \tag{8}$$

where P.V. denotes the Cauchy principal value—we neglect these imaginary parts as they only induce small energy shifts (*Lamb shifts*) that can be reabsorbed in the coherent dynamics, and arrive to

$$\partial_t\tilde{\rho} = \sum_{i,j=1}^{N}\sum_{p,q,r,s} S_{ij}(\omega_{sr})\,u_{ip}u_{iq}u_{jr}u_{js}\Big\{e^{i(\omega_{pq}-\omega_{sr})t}\Big[\sigma_{rs}\tilde{\rho}(t), \sigma_{pq}\Big] + \mathrm{H.c.}\Big\}, \tag{9}$$

with the bath noise-power spectrum

$$S(\omega) = \begin{cases} \pi J(\omega)[n(\omega)+1] & \omega \geqslant 0 \\ \pi J(-\omega)n(-\omega) & \omega < 0 \end{cases}. \tag{10}$$

For a common bath, $S_{ij}^{\rm com}(\omega) = S(\omega)$, while for independent baths, $S_{ij}^{\rm ind}(\omega) = \delta_{i,j}S(\omega)$. Note that $S(0) \equiv \lim_{\omega\to 0^+}S(\omega) = \lim_{\omega\to 0^-}S(\omega)$ is well-defined if $\lim_{\omega\to 0}\dfrac{J(\omega)}{\omega}$ exists.

In the resulting master equation, the terms in which ω_{pq} differs from ω_{sr} oscillate as a function of time t, which can lead to a violation of the positivity of ρ for long times. If the timescale τ_ϕ of the bath-induced system dynamics is much slower than the coherent dynamics, i.e., $\tau_\phi \gg \tau_{\rm SC}$, these terms can be removed by averaging the master equation over a time short compared to τ_ϕ, but long compared to $\tau_{\rm SC}$ [25, 26]. The total bare-

Table 1. List of the incoherent transitions induced by the dephasing interaction, within the secular approximation. Each line shows the label we give to the 'bare' rate γ_{rs} associated with incoherent transitions at frequency difference ω_{sr}. These rates are equal to $\gamma_{rs} = 2S(\omega_{sr})$. The last column indicates to which combinations of states pq, rs each rate applies. Here, the polaritons are labelled as + and −, while the labels d, d', d'', d''' each indicate any of the $N-1$ dark states.

Label	ω_{sr}	$\{pq, rs\}$
γ_e	Ω_R	$\{+-, -+\}$
γ_a	$-\Omega_R$	$\{-+, +-\}$
Γ_e	$\frac{\Omega_R}{2}$	$\{+d, d'+\}, \{d-, -d'\}$ $\{+d, -d'\}, \{d-, d'+\}$
Γ_a	$-\frac{\Omega_R}{2}$	$\{-d, d'-\}, \{d+, +d'\}$ $\{-d, +d'\}, \{d+, d'-\}$
γ_ϕ	0	$\{++, ++\}, \{--,--\}$ $\{dd', d''d'''\}$

molecule width $\gamma = 3.2$ meV [6] presents an upper bound for the bare-molecule dephasing rate $\gamma_\phi \leqslant \gamma$, and thus gives a lower bound for $\tau_\phi \sim 1/\gamma_\phi$. As a consequence, only the *secular* terms $\omega_{pq} = \omega_{sr}$ persist. This *secular approximation*[5] results in a master equation where populations and coherences are decoupled. We note that the secular approximation aids in the interpretation of the different terms that are obtained, but is not required and indeed only used in some of the results shown in the following.

The secular terms are enumerated in table 1, which lists the states $\{pq, rs\}$ connected by transitions with frequency ω_{sr}. For simplicity, we define and label rates associated with each transition frequency, which correspond to twice the noise power spectrum evaluated at ω_{sr}, such that $\gamma_{rs} = 2S(\omega_{sr})$. These are 'bare' rates in the sense that they do not contain the algebraic prefactors from the basis transformation. The factor of two is included so that for the terms where $pq = sr$, we obtain a standard Lindblad term with rate γ_{rs}, i.e.

$$S(\omega_{sr})\{[\sigma_{rs}\tilde{\rho}(t), \sigma_{sr}] + \text{H.c.}\} = \gamma_{rs}\mathcal{L}_{\sigma_{rs}}[\rho], \tag{11}$$

where $\mathcal{L}_X[\rho] = X\rho X^\dagger - \frac{1}{2}\{X^\dagger X, \rho\}$ is a standard Lindblad superoperator. Positive frequencies $\omega_{sr} > 0$ correspond to phonon emission where the system transitions from a higher- to a lower-energy state, while negative frequencies $\omega_{sr} < 0$ correspond to phonon absorption. As shown in table 1, we obtain secular terms connecting the two polaritons ($\gamma_e = 2S(\Omega_R)$, $\gamma_a = 2S(-\Omega_R)$[6]), terms connecting the polaritons with the dark modes ($\Gamma_e = 2S(\Omega_R/2)$, $\Gamma_a = 2S(-\Omega_R/2)$), and terms connecting states with the same energy ($\gamma_\phi = 2S(0)$, equal to the bare-molecule dephasing rate). The latter give pure dephasing for the polaritons $|+\rangle, |-\rangle$, but produce coupling between populations and coherences for all dark states.

The final master equations are obtained by using the properties of the basis transformation matrix u_{ia} to evaluate the algebraic prefactors $\sum_i u_{ip}u_{iq}u_{ir}u_{is}$ (independent baths) and $\sum_{i,j} u_{ip}u_{iq}u_{jr}u_{js}$ (common bath) in equation (9). Specifically, we use that i) the polariton-vibrational mode overlaps are given by $u_{i\pm} = \pm\frac{1}{\sqrt{2N}}$, ii) that dark states are orthogonal to each other ($\sum_i u_{id}u_{id'} = \delta_{d,d'}$), and iii) that dark states are orthogonal to the polaritons ($\sum_i u_{id} = 0$). Note that i and j in the sums are molecule indices (not including the cavity mode), so that $\sum_i u_{ip}u_{iq} = \delta_{p,q}$ is generally not true.

This procedure gives the final secularized master equation for the density operator, given in the Schrödinger picture below. For a common bath with $\phi_{ij}(\tau) = \phi(\tau)$, we find that many terms vanish because of the orthogonality relations, giving

$$\partial_t\rho = -\mathrm{i}[H_s, \rho] + \frac{\gamma_a}{4}\mathcal{L}_{\sigma_{+-}}[\rho] + \frac{\gamma_e}{4}\mathcal{L}_{\sigma_{-+}}[\rho] + \frac{\gamma_\phi}{4}\sum_{p=+,-}\mathcal{L}_{\sigma_{pp}}[\rho] + \gamma_\phi\mathcal{L}_{\mathcal{D}}[\rho], \tag{12}$$

where $\mathcal{D} = \sum_d \sigma_{dd}$ is the projector into the dark-state subspace. The Lindblad terms $\mathcal{L}_X[\rho]$ correspond to incoherent excitation transfer between system eigenstates and are depicted schematically in figure 2(a). A phonon of frequency Ω_R may be emitted transferring an excitation from the upper polariton $|+\rangle$ to the lower

[5] The secular approximation is also sometimes called the *rotating wave approximation*, but should not be confused with the rotating wave approximation performed in the system Hamiltonian in equation (2).

[6] The same γ_a, γ_e are obtained under strong classical driving of a single two-level system [27].

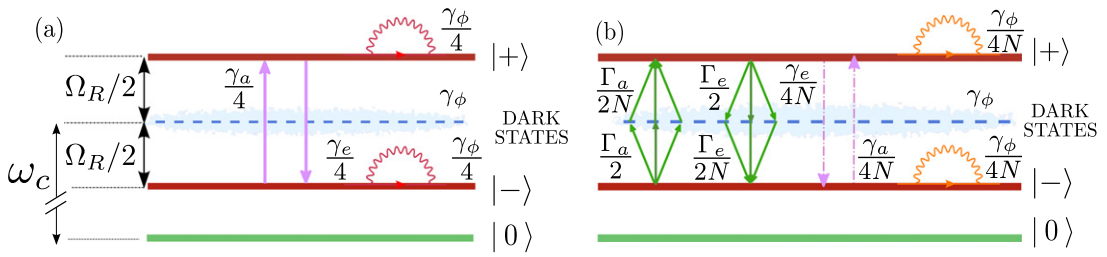

Figure 2. Illustration of the different decay and dephasing mechanisms that emerge from our modeling for the two dephasing scenarios: common bath (panel (a)) or independent baths (panel (b)). The arrows indicate decay processes while wavy lines represent elastic events that produce dephasing. The fuzzy halo around the dark states indicates excitation transfer and dephasing acting within this manifold.

polariton $|-\rangle$, with rate $\gamma_e/4$. Phonon absorption occurs analogously, with characteristic rate $\gamma_a/4$. Furthermore, the polaritons undergo pure dephasing with rate $\gamma_\phi/4$. We note that the factor of 1/4 in these rates can be easily understood: the bare-molecule dephasing interaction (rate γ_ϕ) is reduced by a factor of two for the polaritons, which consists of an equal superposition of molecules and the cavity mode. Since the interaction in the dressed basis couples each polariton not only with itself, but also with the other polariton, the prefactors are reduced by another factor of two. Taking into account the spectral density at the energy difference between the polaritons modifies the rates for transitions between different polaritons (giving γ_a and γ_e instead of γ_ϕ), but the prefactor of 1/4 remains. Finally, the last term in equation (12) corresponds to bare-molecule dephasing for a common bath, but projected into the degenerate dark-state subspace (using $\mathcal{D}\sum_i c_i^\dagger c_i \mathcal{D} = \mathcal{D}$). Remarkably, for the case of a common bath, i.e., long-range bath phonons, the dark states are completely decoupled from the polaritons and the bright state behaves identically to a *single* oscillator interacting with the cavity field.

Turning to the case of independent baths, $\phi_{ij}(\tau) = \delta_{i,j}\phi(\tau)$, we instead find

$$\partial_t\rho = -\mathrm{i}[H_s, \rho] + \frac{\gamma_a}{4N}\mathcal{L}_{\sigma_{+-}}[\rho] + \frac{\gamma_e}{4N}\mathcal{L}_{\sigma_{-+}}[\rho] \tag{13a}$$

$$+\frac{\Gamma_a}{2N}\sum_d\Big(\mathcal{L}_{\sigma_{d-}}[\rho] + \mathcal{L}_{\sigma_{+d}}[\rho]\Big) + \frac{\Gamma_e}{2N}\sum_d\Big(\mathcal{L}_{\sigma_{d+}}[\rho] + \mathcal{L}_{\sigma_{-d}}[\rho]\Big) \tag{13b}$$

$$+\frac{\Gamma_a}{4N}\sum_d\Big([\sigma_{d-}\rho, \sigma_{d+}] - [\sigma_{+d}\rho, \sigma_{-d}] + \mathrm{H.c.}\Big) \tag{13c}$$

$$+\frac{\Gamma_e}{4N}\sum_d\Big([\sigma_{d+}\rho, \sigma_{d-}] - [\sigma_{-d}\rho, \sigma_{+d}] + \mathrm{H.c.}\Big) \tag{13d}$$

$$+\frac{\gamma_\phi}{4N}\sum_{p=+,-}\mathcal{L}_{\sigma_{pp}}[\rho] + \gamma_\phi\sum_i\mathcal{L}_{\mathcal{D}c_i^\dagger c_i\mathcal{D}}[\rho], \tag{13e}$$

which now includes excitation transfer between the polaritons and dark states (Γ_a, Γ_e), driven by phonons of frequency $\Omega_R/2$. While the individual terms are strongly suppressed by the prefactor $1/N$ (with $N \sim 10^{12}$ in the experiments), excitation transfer *into* the dark states still occurs efficiently due to the sum over $N-1$ dark states d. For $N \to \infty$, the *total* population transfer from the polaritons to the dark states thus occurs with rates $\Gamma_a/2$ and $\Gamma_e/2$, as shown in figure 2(b). On the other hand, pure dephasing of the polaritons and direct transitions between them through absorption or emission of phonons of frequency Ω_R play a negligible role within this dephasing scenario, as their rates scale as $1/N$. Additional terms couple between different polariton-dark state coherences (equations (13*c*), (13*d*)), without affecting the populations. Finally, the second term in equation (13*e*) again corresponds to a bare-molecule Lindblad dephasing term that has been restricted to act only within the degenerate dark-state subspace. For $N \to \infty$, equation (13) simplifies to

$$\partial_t\rho = -\mathrm{i}[H_s, \rho] + \frac{\Gamma_a}{2}\bar{\mathcal{L}}_{\mathcal{D}-}[\rho] + \frac{\Gamma_e}{2}\bar{\mathcal{L}}_{\mathcal{D}+}[\rho] + \gamma_\phi\sum_i\mathcal{L}_{\mathcal{D}c_i^\dagger c_i\mathcal{D}}[\rho], \tag{14}$$

where $\bar{\mathcal{L}}_{\mathcal{D}\pm} = \frac{1}{N-1}\sum_d\mathcal{L}_{\sigma_{d\pm}}$ is an averaged Lindblad superoperator inducing equal population transfer from a polariton to all dark states. For large N, the dark states thus act like a sink, and any population transferred to them is trapped and does not further participate in the polariton dynamics.

As is clear from the expressions for the different decay rates, Ω_R is the parameter that controls the interaction between the *dressed* excitation and the phonon bath. Hence the importance of these decoherence mechanisms is dictated by the spectral density evaluated at Ω_R or $\Omega_R/2$. This is in clear contrast to what we would obtain by treating the interaction H_ϕ in the *uncoupled* basis. In that case, the Markov approximation would have resulted in 'standard' Lindblad terms $\gamma_\phi \mathcal{L}_{\sum_i c_i^\dagger c_i}(\rho)$ (common bath) or $\gamma_\phi \sum_i \mathcal{L}_{c_i^\dagger c_i}(\rho)$ (independent baths). In both cases, the dephasing interaction would be totally controlled by just the zero-frequency limit of the spectral density, resulting in an overestimation of the rates $\gamma_{a,e}$ and $\Gamma_{a,e}$. This fact emphasizes the key importance of deriving Lindblad terms in the strongly coupled basis when considering non-flat reservoirs [23].

Apart from the decay and dephasing mechanisms induced by the dephasing-type interactions, which conserve the number of excitations, the excited states may decay through nonradiative molecular decay and cavity losses into the ground state $|0\rangle$. These decay process, which we have neglected in the theory up to now, could be described within the same framework by dissipative coupling with thermal baths (e.g., the photonic modes outside the cavity). However, as the energy shifts induced by the strong coupling are small compared to the transition frequency ($\Omega_R \ll \omega_m$), we can include them through Lindblad terms for the bare cavity and molecular vibrational modes. After removing nonsecular terms in the eigenstate basis, this gives new Lindblad terms with decay rates of $(\gamma_{nr}/2 + \kappa/2)$ for the two polaritons and γ_{nr} for the dark states. We can now obtain the total decay rates by collecting terms that transfer excitations out of each state (i.e., excluding pure dephasing terms), giving

Common bath	Independent baths	
$\Gamma_+^c = \frac{\gamma_{nr}}{2} + \frac{\kappa}{2} + \frac{\gamma_e}{4}$	$\Gamma_+^i = \frac{\gamma_{nr}}{2} + \frac{\kappa}{2} + \frac{N-1}{N}\frac{\Gamma_e}{2} + \frac{\gamma_e}{4N}$	(15*a*)
$\Gamma_-^c = \frac{\gamma_{nr}}{2} + \frac{\kappa}{2} + \frac{\gamma_a}{4}$	$\Gamma_-^i = \frac{\gamma_{nr}}{2} + \frac{\kappa}{2} + \frac{N-1}{N}\frac{\Gamma_a}{2} + \frac{\gamma_a}{4N}$	(15*b*)
$\Gamma_D^c = \gamma_{nr}$	$\Gamma_D^i = \gamma_{nr} + \frac{\Gamma_a + \Gamma_e}{2N}$	(15*c*)

where Γ_+, Γ_-, and Γ_D are the decay rates of the upper polariton, lower polariton, and dark states, respectively. The intrinsic lifetimes for each state in the two bath scenarios are given by $\tau_x^{\mathrm{b}} = 1/\Gamma_x^{\mathrm{b}}$. While the decay of the polaritons is dominated by cavity losses $(\kappa/2)$ for realistic parameters, the upper polariton does have a slightly shorter lifetime than the lower polariton in both scenarios, as $\Gamma_e > \Gamma_a$ and $\gamma_e > \gamma_a$. The exact amount of asymmetry depends on the temperature T and Rabi splitting Ω_R. We note that in contrast to the conceptionally similar model for electronic strong coupling of Canaguier-Durand *et al* [24], our model does not predict a polariton lifetime that is much longer than the cavity mode lifetime.

3. Results

In the following, we apply our theoretical framework to the experimental results of Shalabney *et al* [6]. For the vibrational mode of the *bare* molecules, they report a linewidth of $\gamma = 3.2$ meV, with negligible inhomogeneous broadening. This linewidth has contributions from nonradiative decay and dephasing, $\gamma = \gamma_{nr} + \gamma_\phi$, which can not be distinguished in the absorption spectrum. Although direct information about the weights of non-radiative and dephasing channels is thus not available, dephasing is in general expected to provide a significant contribution for vibrational transitions [14, 15]. Therefore, in our calculations we will use a factor f [$\gamma_\phi = f\gamma$, $\gamma_{nr} = (1-f)\gamma$] to measure the relative importance of the two channels. In this way, the factor η in equation (4), which quantifies the strength of the system-bath coupling, is simply given by $\eta = f\gamma/(2\pi k_{\mathrm{B}} T_0)$ where $T_0 = 300$ K. The cut-off frequency for the thermal bath of low-frequency rovibrational excitations is chosen as $\omega_{\mathrm{cut}} = 6$ meV, corresponding to the range of low-frequency phonon modes in the system [6]. Finally, we use a cavity loss rate of $\kappa = 17$ meV as estimated in [6] through fitting of the transmission spectrum in the strong coupling regime.

We calculate the absorption spectra by introducing a weak driving term, $H_d(t) \sim a e^{-i\omega t} + \mathrm{H.c.}$, which coherently pumps the cavity mode. The density matrix in the steady state, ρ_{ss}, can be calculated in the frame rotating with the driving frequency ω. In this frame, H_d is time-independent, but the system frequencies are shifted and the density matrix ρ_{ss} depends on ω. The absorption spectrum is then obtained as $A(\omega) \propto \mathrm{Tr}[\rho_{ss}(\omega) a]$. For the numerical implementation, we employ the open-source QuTiP package [28].

Figure 3(a) depicts the theoretical absorption spectra for the parameters reproducing the experimental situation, with Rabi splitting $\Omega_R = 20.7$ meV, for the two possible dephasing scenarios analyzed in this work (common or independent baths). Different values of f are tested: $f = 0$, $f = 0.5$ and $f = 1$. Both approaches coincide in the limit $f = 0$ (no dephasing), but their behaviour differs for non-zero f, as can be inferred from the different

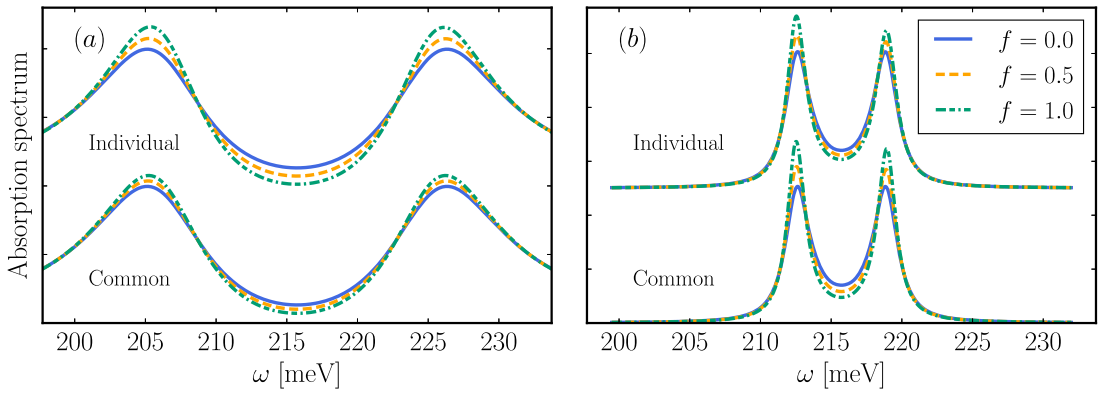

Figure 3. Absorption spectra for the two possible dephasing scenarios as a function of f. In both panels the two sets of curves are offset for a better visualization. In panel (a), the parameters used for the calculations are those reported in [6] (see text), whereas in panel (b), the Rabi splitting and the cavity decay rate are reduced to $\Omega_R = 6.5$ meV and $\kappa = 1$ meV, respectively.

decay rates as rendered in figure 2. The Rabi splitting is much larger than the range of low-frequency vibrations ($\Omega_R \gg \omega_{\text{cut}}$) and, hence, all terms connecting levels with different energies (γ_a, γ_e, Γ_a, Γ_e) are essentially zero. The widths of the polaritons in the absorption spectrum (for $N \to \infty$) are simply given by $\gamma_\pm = \frac{\kappa + \gamma_{nr}}{2} + \frac{\gamma_\phi}{4} = \frac{\kappa}{2} + (1 - \frac{f}{2})\frac{\gamma}{2}$ for a common bath, and $\gamma_\pm = \frac{\kappa + \gamma_{nr}}{2} = \frac{\kappa}{2} + (1 - f)\frac{\gamma}{2}$ for independent baths.

This also implies that for both bath scenarios and within the experimental conditions reported in [6, 7], the ensemble of vibrational modes behaves effectively as just a single collective molecular oscillator, the bright state, coupled to the cavity mode. Consequently, the dark modes are effectively decoupled from the system dynamics under external driving. We note here that the fit used to extract the cavity width κ from the experimental data in [6] is performed under strong coupling (using a transfer matrix method). Thus, the change of linewidths predicted by our model would already be present in the observed spectra, and is consequently absorbed in the extracted cavity linewidth. This unfortunately precludes a direct test of our model based on the experimental absorption data, for which the *bare* cavity linewidth would need to be available.

Furthermore, it is interesting to note that in the case of individual baths, the dephasing contributions to the polariton modes are completely suppressed, analogous to the well-known suppression of inhomogeneous broadening under strong coupling [29]. This can be understood by the fact that dephasing and inhomogeneous broadening are closely related, corresponding respectively to temporal fluctuations or to a static distribution of the transition energies.

The dark modes could play a bigger role in a situation with smaller Rabi splitting, for which, in order to still achieve strong coupling, the cavity losses also need to be reduced as compared to the experiments (e.g., by using thicker mirrors). The resulting absorption spectra are shown in figure 3(b), for the same parameters as in figure 3(a) but now with $\kappa = 1$ meV and $\Omega_R = 6.5$ meV. In both bath scenarios, a slight asymmetry between upper and lower polariton is now noticeable, as the emission of phonons from the upper polariton (γ_e, $\Gamma_e \propto n(\omega) + 1$) is more likely than the absorption of phonons in the lower polariton (γ_a, $\Gamma_a \propto n(\omega)$). However, as the involved transition frequencies are smaller than the thermal energy ($k_B T = 25.9$ meV for $T = 300$ K), the thermal occupation $n(\omega)$ is significant and the rates for phonon emission and absorption are comparable. Furthermore, although the phenomenology in the observed absorption spectra is quite similar in both dephasing scenarios, with a reduction of the polariton linewidths for increasing dephasing f, the underlying physics are now quite distinct. This is demonstrated clearly when inspecting the population dynamics, shown in figure 4 for the case of the upper polariton being initially excited. In both cases, the dynamics are dominated initially by the fast decay of the upper polariton through cavity losses (rate $\kappa/2$, cf equation (15)). However, the more interesting aspect is the dynamics within the excited subspace: for the common bath, shown in figure 4(a), the dark states are completely decoupled from the dynamics and population is only transferred between the polaritons. In contrast, in the case of independent baths, shown in figure 4(b), the excited population is quite efficiently transferred from the upper polariton to the dark states, resulting in a fast rise of the dark state population. The dark states subsequently decay through nonradiative molecular loss (γ_{nr}, cf equation (15)), which is smaller than the polariton loss rate. We also note that the small but visible population transfer to the lower polariton only shows up because we show results for $N = 100$, not in the limit $N \to \infty$ (cf equation (14)).

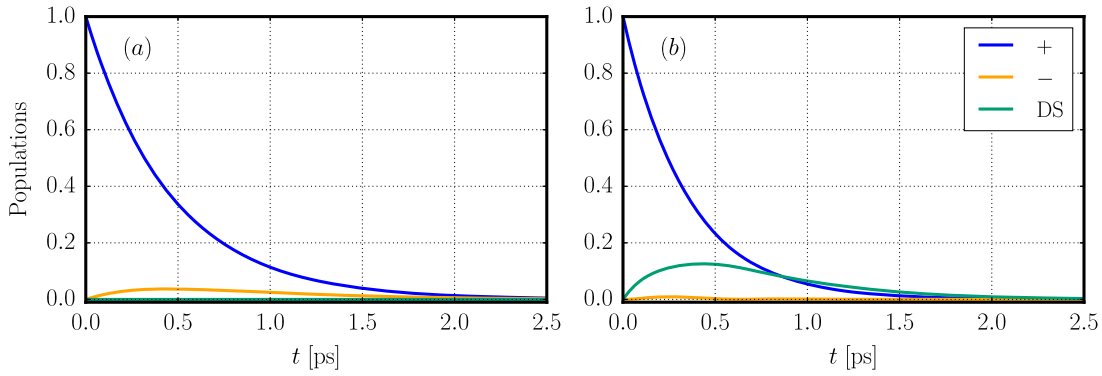

Figure 4. Population dynamics starting from the initially excited upper polariton $|+\rangle$ for the two possible dephasing scenarios: (a) common bath and (b) independent baths. The parameters are the same as in figure 3(b), with $f = 0.5$ and $N = 100$. Each panel shows the upper polariton (+) and lower polariton (−) populations, as well as the total population in all dark states (DS), given by $\mathrm{Tr}(\mathcal{D}\rho)$.

4. Conclusions

In summary, by using a fully quantum framework we have studied in detail the phenomenon of collective strong coupling when an ensemble of molecular vibrational modes interacts with a cavity EM mode, as realized experimentally in two recent papers [6, 7]. We have demonstrated that dephasing-type interactions with a thermal bath of background modes in such a system have to be treated beyond the usual Lindblad approximation in order to represent the effects of the spectral density of bath modes correctly. We have investigated two 'extreme' scenarios for the bath, with either a common bath for all molecules, or independent baths for each molecule. For the experimentally relevant parameters, we find that the dark modes are almost totally decoupled from the polaritons in both scenarios, and the bright state behaves almost like a single isolated oscillator. Our findings thus suggest that this type of system is an ideal and simple platform to explore the exciting possibilities of cavity optomechanics at room temperature.

Acknowledgments

This work has been funded by the European Research Council (ERC-2011-AdG proposal No. 290981), by the European Union Seventh Framework Programme under grant agreement FP7-PEOPLE-2013-CIG-618229, and the Spanish MINECO under contract MAT2011-28581-C02–01.

References

[1] Gigan S, Böhm H R, Paternostro M, Blaser F, Langer G, Hertzberg J B, Schwab K C, Bäuerle D, Aspelmeyer M and Zeilinger A 2006 Self-cooling of a micromirror by radiation pressure *Nature* **444** 67
[2] Arcizet O, Cohadon P-F, Briant T, Pinard M and Heidmann A 2006 Radiation–pressure cooling and optomechanical instability of a micromirror *Nature* **444** 71
[3] Schliesser A, Del'Haye P, Nooshi N, Vahala K J and Kippenberg T J 2006 Radiation pressure cooling of a micromechanical oscillator using dynamical backaction *Phys. Rev. Lett.* **97** 243905
[4] Aspelmeyer M, Kippenberg T J and Marquardt F 2014 Cavity optomechanics *Rev. Mod. Phys.* **86** 1391
[5] Aspelmeyer M, Kippenberg T J and Marquardt F (ed) 2014 *Cavity Optomechanics* (Berlin: Springer) (doi:10.1007/978-3-642-55312-7)
[6] Shalabney A, George J, Hutchison J, Pupillo G, Genet C and Ebbesen T W 2015 Coherent coupling of molecular resonators with a microcavity mode *Nat. Commun.* **6** 5981
[7] Long J P and Simpkins B S 2015 Coherent coupling between a molecular vibration and Fabry-Perot optical cavity to give hybridized states in the strong coupling limit *ACS Photonics* **2** 130
[8] Lidzey D G, Bradley D D C, Skolnick M S, Virgili T, Walker S and Whittaker D M 1998 Strong exciton-photon coupling in an organic semiconductor microcavity *Nature* **395** 53
[9] Schwartz T, Hutchison J A, Genet C and Ebbesen T W 2011 Reversible switching of ultrastrong light-molecule coupling *Phys. Rev. Lett.* **106** 196405
[10] Kéna-Cohen S, Maier S A and Bradley D D C 2013 Ultrastrongly coupled exciton-polaritons in metal-clad organic semiconductor microcavities *Adv. Opt. Mater.* **1** 827
[11] Bellessa J, Bonnand C, Plenet J C and Mugnier J 2004 Strong coupling between surface plasmons and excitons in an organic semiconductor *Phys. Rev. Lett.* **93** 036404
[12] Törmä P and Barnes W L 2015 Strong coupling between surface plasmon polaritons and emitters: a review *Rep. Prog. Phys.* **78** 013901
[13] Michetti P, Mazza L and la Rocca G C 2015 Strongly coupled organic microcavities *Organic Nanophotonics* (*Nano-Optics and Nanophotonics*) ed Y S Zhao (Berlin: Springer) pp 39–68
[14] Oxtoby D W 1979 Dephasing of molecular vibrations in liquids *Adv. Chem. Phys.* **40** 1
[15] Tanimura Y and Mukamel S 1993 Two-dimensional femtosecond vibrational spectroscopy of liquids *J. Chem. Phys.* **99** 9496

[16] Wangsness R K and Bloch F 1953 The dynamical theory of nuclear induction *Phys. Rev.* **89** 728
[17] Redfield A G 1955 Nuclear magnetic resonance saturation and rotary saturation in solids *Phys. Rev.* **98** 1787
[18] González-Tudela A, Huidobro P A, Martín-Moreno L, Tejedor C and García-Vidal F J 2014 Reversible dynamics of single quantum emitters near metal-dielectric interfaces *Phys. Rev.* B **89** 041402(R)
[19] Delga A, Feist J, Bravo-Abad J and Garcia-Vidal F J 2014 Quantum emitters near a metal nanoparticle: strong coupling and quenching *Phys. Rev. Lett.* **112** 253601
[20] Gardiner C W and Zoller P 2004 *Quantum Noise: A Handbook of Markovian and Non-Markovian Quantum Stochastic Methods with Applications to Quantum Optics* (Berlin: Springer)
[21] Breuer H-P and Petruccione F 2007 *The Theory of Open Quantum Systems* (Oxford: Oxford University Press) p 636
[22] Gerald Mahan D 2000 *Many-Particle Physics* (Boston, MA: Springer) (doi:10.1007/978-1-4757-5714-9)
[23] Carmichael H J and Walls D F 1973 Master equation for strongly interacting systems *J. Phys. A: Math. Nucl. Gen.* **6** 1552
[24] Canaguier-Durand A, Genet C, Lambrecht A, Ebbesen T W and Reynaud S 2015 Non-Markovian polariton dynamics in organic strong coupling *Eur. Phys. J.* D **69** 24
[25] Dümcke R and Spohn H 1979 The proper form of the generator in the weak coupling limit *Z. für Phys.* B **34** 419
[26] Spohn H 1980 Kinetic equations from Hamiltonian dynamics: Markovian limits *Rev. Mod. Phys.* **52** 569
[27] Eastham P R, Spracklen A O and Keeling J 2013 Lindblad theory of dynamical decoherence of quantum-dot excitons *Phys. Rev.* B **87** 195306
[28] Johansson J R, Nation P D and Nori F 2013 QuTiP 2: a python framework for the dynamics of open quantum systems *Comput. Phys. Commun.* **184** 1234
[29] Houdré R, Stanley R P and Ilegems M 1996 Vacuum-field Rabi splitting in the presence of inhomogeneous broadening: resolution of a homogeneous linewidth in an inhomogeneously broadened system *Phys. Rev.* A **53** 2711